Theoretical spectrum of noisy optical pulse trains

B. Lacaze[1,*] and M. Chabert[2]

[1]Télécommunications Spatiales et Aéronautiques laboratory 14-18 Port Saint Etienne 31000 Toulouse France

[2]University of Toulouse INPT/ENSEEIHT / IRIT 2, rue Camichel BP 7122-F-31071 Toulouse Cedex 7 France

*Corresponding author: bernard.lacaze@tesa.prd.fr

Received 12 December 2007; revised 17 April 2008; accepted 18 April 2008;
posted 9 May 2008 (Doc. ID 90816); published 11 June 2008

The intensity of an ideal optical pulse train is often modeled as an exact periodic repetition of a given pulse-shape function with constant amplitude and width. Therefore, the ideal intensity power spectrum is a pure line power spectrum. However, spontaneous-emission noise due to amplification media, electronic noise due to modulators, or even intentional modulations result in period-to-period fluctuations of the pulse amplitude, width, or arrival time. The power spectrum of this so-called noisy optical pulse train is then composed of a line spectrum added to a band spectrum. This study shows that the optical pulse train intensity is cyclostationary under usual assumptions on the fluctuations. This property allows us to derive the exact optical pulse train power spectrum. A general closed-form expression that takes into account the three noise manifestations (jitter, amplitude, and width modulations) is provided. Particular expressions are given for usual cases of interest such as the jitter and amplitude modulation model, for given fluctuation probability distributions, and pulse-shape functions. © 2008 Optical Society of America

OCIS codes: 140.7090, 140.4050.

1. Introduction

Periodically spaced short-duration light pulses called optical pulse trains are currently used in many applications. Modulated optical pulse trains allow high bit-rate transmissions through optical fibers [1,2]. Optical pulse trains are of current interest for optic measurement techniques such as time-resolved spectroscopy [3] or electro-optic sampling [4]. Time-resolved spectroscopy consists of probing the chemical, biological, or physical characteristics of a medium by short-duration light pulses [3]. Electro-optic sampling employs optical pulse trains to provide noninvasive measurements of fast electronic devices and circuits [4]. The optical pulse train characterization is of great importance for the calibration of coherent light sources such as optical parametric oscillators [5]. Optical parametric oscillators produce coherent light with broader frequency tunability than conventional laser sources and cover transmission bands from the visible to the far infrared spectrum, motivating research and industrial interest.

All these applications require an accurate tailoring and control of the optical pulse train intensity. According to Ref. [6], the observation of the output fluctuations is used as a criterion for the correct adjustment of the laser modulation frequency, for instance. The ideal intensity model consists in the exact periodic repetition of a given short-duration pulse-shape function. We study the influence of fluctuations of the pulse arrival time (jitter), width (random widening or width modulation), and amplitude (amplitude modulation) on the measured intensity. Note, for simplicity, that fluctuations of the carrier frequency due to propagation in dispersive media are generally not considered in the literature (see Refs. [6–8], for instance). However, this simplified model provides a convenient approximation on large signal segments for a slowly varying carrier frequency. The considered fluctuations may come from spontaneous-emission noise due to amplification media or electronic noise due to modulators. For instance, the jitter is due to a mismatching between the laser reference frequency and the cavity length,

0003-6935/08/183231-10$15.00/0

to the reference oscillator noise, or to spontaneous-emission noise in the case of actively mode-locked lasers [7]. The fluctuations can carry some information of interest in the case of electro-optic measurements or optic communications. For instance, usual fiber optic modulations modify either the pulse position (pulse-point modulation) [1], width (pulse-width modulation) [2], or amplitude (amplitude-shift keying) to code the transmitted information.

Intensity fluctuations are characterized through experiments by shining the laser light on a photodetector. This characterization is generally performed directly on the measured intensity. However, the so-called second-harmonic method measures the frequency-doubled intensity obtained by a nonlinear processing of the original optical pulse train [6,8]. The second-harmonic method amounts to the measurement of higher-order correlations [6]. For both methods, the photocurrent at the output of the photodetector is spectrally analyzed. The bandwidth of the measurement device composed of the photodetector and the spectrum analyzer is generally far narrower than the signal bandwidth [6]. Consequently, the intensity or frequency-doubled intensity spectra are measured in short frequency windows around given spectrum lines, also called harmonics [8]. The comparison of the measurements with theoretical expressions aims at characterizing jitter, width, and amplitude modulations [9]. Approximations of the spectrum of the noisy optical pulse train intensity have been obtained using the Maclaurin series [9,10] and polynomial regression curves [11], under the assumption of small fluctuations. In Ref. [6], assuming that width modulation can be neglected, the jitter and the amplitude modulation are estimated from approximations of the intensity power spectrum when the product between the pulse width and the frequency is within a particular range. However, this condition is not met for particular laser width specifications and measurement device bandwidths [9].

The aim of this study is to provide the exact expression of the noisy optical pulse train intensity spectrum in the presence of the three fluctuations (jitter, width, and amplitude modulations) and in any frequency range.

Section 2 considers a general random model for the optical pulse train intensity. This model takes into account jitter, width, and amplitude modulations. Under realistic assumptions on the pulse properties and on the fluctuations, the measured intensity is shown to be cyclostationary. Section 3 expresses the power spectrum in closed form as a function of the fluctuation probability distributions. Section 4 provides simplified expressions for particular cases of interest: jitter and amplitude modulation model, width modulation model with given fluctuation probability distributions, and pulse-shape functions. The three types of pulse fluctuations are characterized through their spectral signatures. Conclusions are reported in Section 5.

2. Noisy Optical Pulse Train Model

The most general model of the optical pulse train considers random fluctuations of the pulse amplitude, arrival time, and width [9]. The measured intensity of the optical pulse train is given by

$$I(t) = \sum_{n=-\infty}^{\infty} A_n f\left(\frac{t - t_0 - J_n - nT}{W_n}\right), \quad \forall\, t \in \mathbb{R} \qquad (1)$$

where:

– T is the averaged train period. Let $T = 1$ for simplicity and without any loss of generality.

– A_n, W_n, and J_n model the amplitude and width modulations and the jitter, respectively. For simplicity, let $E[W_n] = 1$ and $E[J_n] = 0$, where $E[.]$ denotes mathematical expectation (mean value of the random variable through experiments). These three random variables are possibly correlated.

– $f(.)$ is the shape function or profile of the pulse intensity as observed by the measurement device. The function is assumed regular enough for further derivation purposes and the intensity normalization leads to

$$\int_{-\infty}^{\infty} f(t)\mathrm{d}t = 1. \qquad (2)$$

In practice, the light pulse duration is finite and short with respect to the period. Consequently, $f(t)$ is assumed to have a compact support (the set of t values for which $f(t) \neq 0$) included in a small interval $\left[\frac{-\Delta t}{2}, \frac{\Delta t}{2}\right]$ such that $\Delta t \leq 10^{-3}$ [11,12]. The averaged pulse duration is thus smaller than Δt. Note that the Δt value is normalized with respect to the pulse period. In experiments, Δt is usually expressed in femtoseconds, picoseconds, or nanoseconds. A very small averaged pulse duration with respect to the averaged period prevents consecutive pulses from overlapping under reasonable jitter and width modulation. This study considers slow intensity fluctuations with respect to the pulse duration. The pulse shape $f(t)$ then remains constant from pulse to pulse. The resulting model is the so-called constant shape laser noise model studied in Ref. [9] as opposed to the noise burst model in Ref. [6].

– t_0 is a shift parameter such that $f(t - t_0 - n)$ is far from the boundaries of the nth time period $[n, n+1[$. Appendix A shows that $f\left(\frac{t-t_0-J_n-n}{W_n}\right)$ remains in the time period $[n, n+1[$ under reasonable jitter and amplitude modulation if $\int_{-\infty}^{\infty} tf(t)\mathrm{d}t = 0$.

Finally, the optical pulse train is composed of one pulse with particular shift, amplitude, and width per time period. The infinite sum in Eq. (1) then simplifies to a single term expression given by

$$I(t) = A_{\bar{t}} f\left(\frac{t - t_0 - J_{\bar{t}}}{W_{\bar{t}}}\right), \quad \forall\, t \in \mathbb{R}, \qquad (3)$$

where $\bar{t}$ is the integer part and $\underline{t}$ is the fractional part of t: $t = \bar{t} + \underline{t}, \bar{t} \in \mathbb{Z}$ and $0 \le \underline{t} < 1$. The intensity can be decomposed into a sequence of random processes $\mathbf{G} = \{G_n(t), \quad n \in \mathbb{Z}\}$ defined by

$$G_n(t) = A_n f\left(\frac{t - t_0 - J_n}{W_n}\right), \tag{4}$$

where $G_n(t)$ models the intensity of the pulse included in the nth time period $[n, n+1[$. Under physically plausible assumptions, the sequence $\mathbf{G}$ satisfies the four following conditions:

$$G_n(t) = 0, \quad t \notin [0,1], \tag{5}$$

$$E[G_n(t)] = \alpha(t) \text{ is independent of } n, \tag{6}$$

$$E[G_n(u)G_{n+m}(v)] = \beta_m(u,v) \text{ is independent of } n, \tag{7}$$

$$\beta_m^0(u,v) = \beta_m(u,v) - \alpha(u)\alpha(v) \underset{m\to\infty}{\to} 0 \text{ uniformly in } (u,v). \tag{8}$$

Condition (5) assumes nonoverlapping pulses. Condition (8) means asymptotic uncorrelatedness of $\mathbf{G}$ elements. Conditions (6) and (7) result in a cyclostationary process $I(t)$ [13]. Indeed, the conditions imply that the two following quantities are periodic with respect to the time variable t:

$$E[I(t)] = E\left[A_{\bar{t}} f\left(\frac{\underline{t} - t_0 - J_{\bar{t}}}{W_{\bar{t}}}\right)\right] = \alpha(\underline{t}) E[I(t)I(t-\tau)]$$
$$= \beta_{\overline{t-\tau}-\bar{t}}(\underline{t}, \underline{t} - \tau).$$

This cyclostationarity property allows for the exact derivation of the power spectrum of $I(t)$. Obviously, one could envision, for instance, specific modulators leading to more complex pulse to pulse relationships than Eqs. (7) and (8). However, this cyclostationarity property, also considered in Ref. [8], seems reasonable in most practical applications. The following section provides a general closed-form expression of the intensity power spectrum as a function of the jitter, amplitude, and width modulation characteristic functions.

3. General Formulation of the Intensity Power Spectrum

First let us assume that the Fourier transform and Fourier series are well defined for the considered mathematical entities and that the Parseval theorem holds. The power spectrum of the measured intensity is defined as the Fourier transform of its temporal average correlation [6,8]:

$$\langle I(t)I(t+\tau)\rangle = \lim_{L\to\infty} \frac{1}{L} \int_{-\frac{L}{2}}^{\frac{L}{2}} I(t)I(t+\tau)\mathrm{d}t.$$

Obviously, when the integral converges, the temporal average correlation is independent of t. Let $\hat{I}(t)$ denote $I(t+\Phi)$ with Φ uniformly distributed over $[0,1]$. If $I(t)$ is wide sense cyclostationary, $\hat{I}(t)$ is wide sense stationary [13]. Assuming ergodicity of the process $I(t)$, the temporal average $\langle I(t)I(t+\tau)\rangle$ identifies with the second order moment $K(\tau) = E[\hat{I}(t)\hat{I}(t+\tau)]$. The power spectrum $s(\omega)$ of $I(t)$ can then be defined [14,15] by

$$K(\tau) = \int_{-\infty}^{\infty} e^{i\omega\tau} s(\omega)\mathrm{d}\omega.$$

Let $\tilde{x}(\omega) = \int_{-\infty}^{\infty} x(t)e^{-i\omega t}\mathrm{d}t$ denote the Fourier transform of function $x(t)$, $t \in \mathbb{R}$. Appendix B provides the following closed-form expression of the $I(t)$ power spectrum [16]:

$$s(\omega) = s_B(\omega) + s_L(\omega) \text{with:}$$
$$\begin{cases} s_B(\omega) = & \frac{1}{2\pi}\sum_{n=-\infty}^{\infty} \tilde{\beta}_n^0(\omega) e^{i\omega n}, \\ s_L(\omega) = & \sum_{n=-\infty}^{\infty} |\tilde{\alpha}(2\pi n)|^2 \delta(\omega - 2\pi n), \end{cases} \tag{9}$$

where $\delta(\omega)$ denotes the Dirac function, β_n^0 and α have been defined in Eqs. (6) and (8), $s_B(\omega)$ refers to the band spectrum, and $s_L(\omega)$ corresponds to the line spectrum. The line spectrum is determined by the first-order moment of the pulse, whereas the correlation between pulses defines the band spectrum. The spectrum closed-form expression given in Eq. (9) is the main result of this paper. This expression is very general since it is valid for any noise distribution and in any frequency range. As explained in the introduction, the literature only provides approximations for simplified noise configurations and in particular frequency ranges. In the following, the band and line spectrum are derived from the provided general expressions for some usual simplified models: the deterministic optical pulse train, the amplitude and jitter case, and, finally, the width modulation case.

4. Specific Expressions of the Intensity Power Spectrum

The three fluctuations are generally not considered simultaneously in applications. For instance, Ref. [17] considers only jitter and amplitude modulation, whereas Ref. [10] considers only jitter and width modulation. According to Ref. [9], width modulation cannot be neglected in the case of Nd:YLF (neodymium doped: yttrium lithium fluoride) lasers. Reference [7] focusses on jitter in phase-encoded sampling systems as they are insensitive to amplitude and

width modulations. Moreover, the hypotheses on the correlation between fluctuations differ according to the laser or to the measurement frequency band. According to Ref. [11], for gain-switched lasers, the different fluctuations are significantly correlated. According to Ref. [8], the correlation between width and amplitude correlation is not negligible for mode-locked lasers, whereas the correlation between jitter and amplitude modulation is small. This significant correlation between amplitude and width modulations has been experimentally observed at low frequencies. This phenomenon can be explained by the pulse energy conservation in this frequency range for mode-locked lasers [10]; pulse amplitude fluctuations are exactly compensated by pulse-width fluctuations to guarantee the absence of pulse energy fluctuations in mode-locked laser operation. The pulse energy conservation does not hold in the frequency range of relaxation oscillation noise. This noise reveals an energy transfer from the intracavity optical power to the population inversion of erbium ion states [10]. Indeed, since this population inversion occurs under optical excitation, a part of the pulse energy is absorbed. Finally, the origin of the fluctuations and their relative importance is widely different for the various types of laser and the different applications. This results in many possible simplified models.

The following subsections provide simplified expressions in some particular cases of interest.

A. Deterministic Optical Pulse Train

First consider the ideal case of a deterministic periodic intensity. In this case, A_n, J_n, and W_n are degenerate random variables. Let $A_n = W_n = 1$ and $J_n = 0$ with probability 1. In this case, the average temporal correlation of the intensity can be developed in a Fourier series. The Parseval theorem then yields

$$\begin{cases} s_B(\omega) = & 0, \\ s_L(\omega) = & \sum_{n=-\infty}^{\infty} |\widetilde{f}(2\pi n)|^2 \delta(\omega - 2\pi n). \end{cases} \tag{10}$$

The intensity power spectrum is perfectly defined by the Fourier series coefficients of the pulse-shape function. Note that other fixed values for A_n and W_n would lead to slightly different line weights, whereas a different value of J_n would have no influence. For a small pulse width, the line weight $|\widetilde{f}(2\pi n)|^2$ decreases very slowly with n. For example, a rectangular pulse of width $\Delta t = 10^{-3}$ leads to $|\widetilde{f}(0)|^2/|\widetilde{f}(2\pi.100)|^2 = 1.0336$. An ideal optical pulse train is the convolution between a pulse shape and an impulse train in the time domain. In the frequency domain, since the impulse train transforms to another impulse train, the ideal optical pulse train is the multiplication between a pulse train and the pulse-shape function Fourier transform. Figure 1 displays the relative decrease $\log\left[\frac{s(0)-s(\omega)}{s(0)}\right]$ of the power spectrum of a deterministic optical pulse train with a rectangular pulse of width $\Delta t = 10^{-3}$ from the first to the twenty-fifth harmonic. A logarithmic scale must be used to observe the power spectrum variations because of the very slow decrease of the pulse-shape Fourier transform. Indeed, with a linear scale, the power spectrum appears as a pure impulse train with constant amplitude. In the following, the theoretical expression (10) and the associated figure can be used as references to characterize the different fluctuation effects.

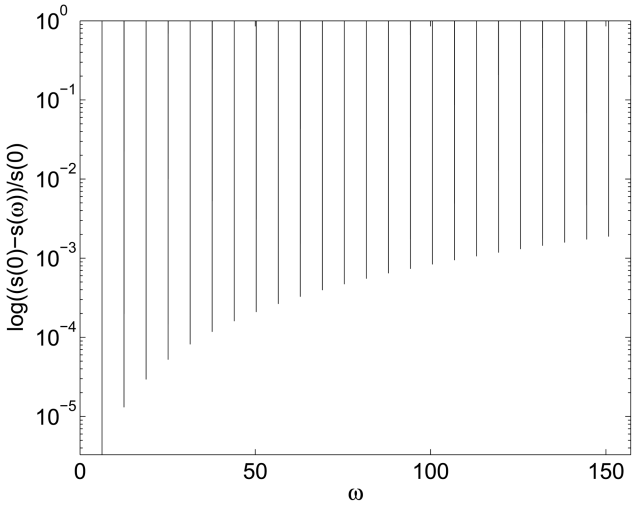

Fig. 1. Relative variations of the intensity power spectrum of a deterministic optical pulse train in logarithmic scale over the first 25 harmonics ($\Delta t = 10^{-3}$ and $T = 1$)

B. The Amplitude Modulation and Jitter Case

The amplitude modulation and jitter model is the most commonly used in applications [10,17–19]. This model is particularly appropriate to characterize the defects of laser sources induced by pump-power or cavity-length fluctuations for mode-locked lasers [18]. In this case, the pulse amplitude fluctuations results in pulse energy fluctuations. Moreover, modulations of the pulse position and the amplitude are the most commonly used in fiber communications [1].

Under amplitude modulation and jitter only, the line and band intensity power spectra in Eq. (9) become

$$\begin{cases} s_B(\omega) = & \frac{1}{2\pi}\sum_{n=-\infty}^{\infty}[|\widetilde{f}|^2.(\phi_n - |\psi|^2)](\omega)e^{in\omega}, \\ s_L(\omega) = & \sum_{n=-\infty}^{\infty}[|\widetilde{f}.\psi|^2](2\pi n)\delta(\omega - 2\pi n). \end{cases} \tag{11}$$

$\psi(\omega)$ and $\phi_n(\omega)$ denote the characteristic functions of the jitter and of the amplitude modulation:

$$\begin{aligned} \psi(\omega) &= E\left[A_k e^{i\omega J_k}\right] \quad \text{and} \quad \phi_n(\omega) \\ &= E\left[A_{n+m}A_m e^{i\omega(J_{n+m}-J_m)}\right]. \end{aligned} \tag{12}$$

As illustrated by experimental measurements in Ref. [17], each spectrum component contains a line

plus a pedestal resulting from both amplitude modulation and jitter. Moreover, Eq. (11) shows that the line weight differs from those obtained in the deterministic case. When the jitter and amplitude vary slowly with respect to the average train period, the amplitude modulation widens the harmonics with an ω-invariant ratio since $\phi_n(\omega) \simeq 1$. On the contrary, the effect of jitter is negligible for low-order harmonics and prevails for higher-order harmonics. Indeed, according to measurements in Ref. [11] and to spectrum Taylor expansions in Ref. [6], the amplitude modulation effect is constant other all harmonics of indices l, whereas the jitter effect is proportional to l^2. Consequently, the jitter (respectively, amplitude modulation) can be characterized by measuring the optical pulse train spectrum at high (respectively, low) frequency. The correlation between jitter and amplitude modulation have been studied in Refs. [18,19].

The following subsections consider jitter and amplitude modulation individually providing simplified spectrum expressions:

1. *The Amplitude Modulation Case*

Consider the pure amplitude modulation model with no jitter nor width modulation, namely $J_n = 0$ and $W_n = 1$ with probability 1 and A_n is random. This model is used in the field of digital communications. For example, the ubiquitous Manchester code, also called biphase, corresponds to $f(t) = 1$ for $0 < t < 1/2$ and -1 for $1/2 < t < 1$, while the uncorrelated $\{A_n\}_{n\in\mathbb{Z}}$ sequence is such that $A_n = 1$ with probability p and $A_n = -1$ with probability $1-p$ [20,21]. For the sake of simplicity, communication models generally consider independent identically distributed sequences as studied in the following:

The Independent Amplitude Modulation Case
First consider the case where A_n is an independent identically distributed random variable with $E[A_n] = m_A$, $VarA_n = \sigma_A^2 > 0$. In this case, the general expression in Eq. (9) simplifies to

$$\begin{cases} s_B(\omega) = & \frac{1}{2\pi}\sigma_A^2|\widetilde{f}(\omega)|^2, \\ s_L(\omega) = & m_A^2 \sum_{n=-\infty}^{\infty} |\widetilde{f}(2\pi n)|^2 \delta(\omega - 2\pi n). \end{cases} \tag{13}$$

The band spectrum values for $\omega = 2\pi n$, $n \in \mathbb{Z}$ are proportional to the line spectrum values at the same angular frequencies. The resulting spectrum is a sequence of harmonics (the line spectrum) with a broad base indicating that the laser is not perfectly mode-locked and thus submitted to fluctuations (the band spectrum) [6]. Assume that the total power is equal to $(\sigma_A^2 + m_A^2)\int_0^1 f^2(t)\mathrm{d}t = \sigma_A^2 + m_A^2 = 1$. Amplitude modulation attenuates the line spectrum with respect to the deterministic case ($\sigma_A = 0$, $m_A = 1$). Figure 2 displays the optical pulse train spectrum for an independent amplitude modulation with $m_A = \sigma_A^2 = 0.5$ with the same rectangular pulse as in the deterministic case. The line weights are smaller than in the deterministic case, whereas an approximately constant pedestal has been added. Note that the line and band spectra decrease at the same rate as in the deterministic case, which is very slow with respect to the frequency observation window.

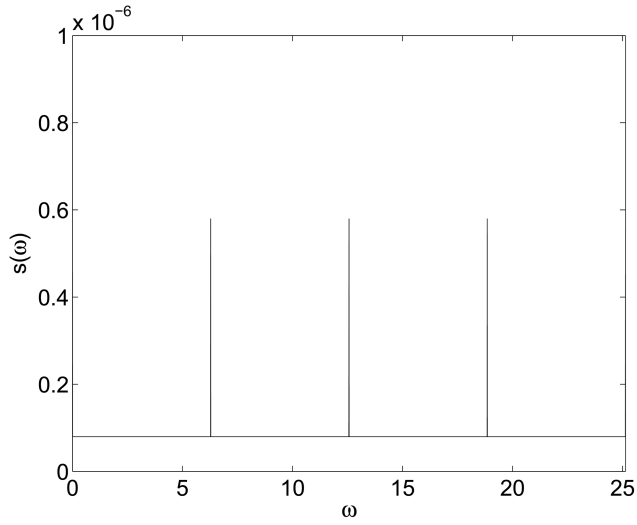

Fig. 2. Intensity power spectrum (first four harmonics) of an optical pulse train submitted to independent amplitude modulation with unit energy ($\Delta t = 10^{-3}$, $T = 1$, $E[A^2] = 1$).

The Dependent Amplitude Modulation Case
Now consider the case of a dependent amplitude modulation with covariance sequence $\{\rho_A(n)\}_{n\in\mathbb{Z}}$:

$$\begin{cases} \rho_A(n) = E[A_k A_{k+n}] - m_A^2 = \int_{-\pi}^{\pi} s_{\mathfrak{A}}(\omega) e^{in\omega} \mathrm{d}\omega, \\ s_A(\omega) = \frac{1}{2\pi}\sum_{n=-\infty}^{\infty} \rho_A(n) e^{-in\omega}. \end{cases}$$

$s_{\mathfrak{A}}(\omega)$ is the power spectrum of the centered sequence $\mathfrak{A}_n = A_n - m_A$, $n \in \mathbb{Z}$ [15]. Thus, $s_{\mathfrak{A}}(\omega)$ is a 2π-periodic function of ω. In this case, Eq. (9) yields

$$\begin{cases} s_B(\omega) = & [s_{\mathfrak{A}}.|\widetilde{f}|^2](\omega), \\ s_L(\omega) = & m_A^2 \sum_{n=-\infty}^{\infty} |\widetilde{f}(2\pi n)|^2 \delta(\omega - 2\pi n). \end{cases} \tag{14}$$

If the sequence $\rho_A(n)$ decreases slowly when n goes from 0 to infinity, $s_{\mathfrak{A}}(\omega)$ concentrates around the points $\omega = 2n\pi$. Consequently, the correlated amplitude modulation can be characterized by the widening of the ideal spectrum lines. This phenomenon can be observed on experimental measurements displayed in Ref. [6]. The band-spectrum concentration around the lines allows for amplitude modulation characterization even in the short frequency window available in practical measurements. Figure 3 displays the intensity power spectrum in the case of dependent amplitude modulation. The pulse remains rectangular with duration $\Delta t = 10^{-3}$; A_n is modeled as an autoregressive process [13] with parameters [1–0.5] and $m_A^2 = 0.5$. The band-spectrum concentration around the lines can be observed on this figure. However, note that the model of amplitude modulation only is oversimplified to fit all applications.

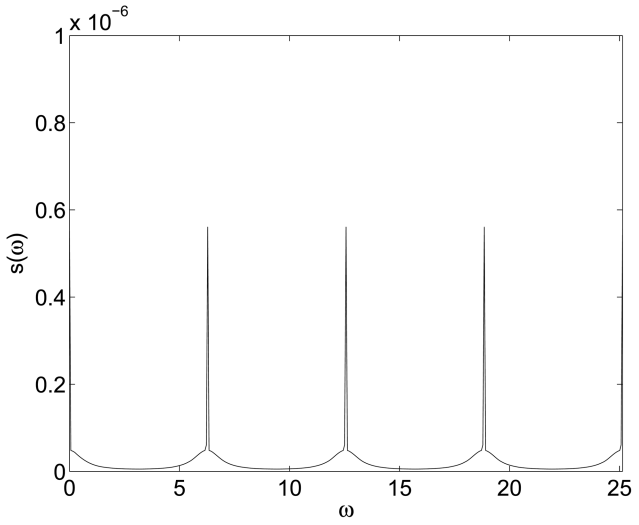

Fig. 3. Intensity power spectrum (first four harmonics) of an optical pulse train submitted to dependent amplitude modulation modeled by an autoregressive process with parameter [1 −0.5] ($\Delta t = 10^{-3}$, $T = 1$, $E[A]^2 = 0.5$).

Indeed, since $s_{\mathfrak{A}}(\omega)$ is 2π-periodic, Eq. (14) does not explain the simultaneous band spectrum increase and line spectrum decrease observed in some real measurements [22]. As shown in the following subsections, jitter can explain this power spectrum behavior.

2. *The Jitter Case*

Now assume that there is no amplitude nor width modulation: $A_n = W_n = 1$ with probability 1. Some applications such as electro-optic sampling or time-resolved spectroscopy require a very accurate jitter characterization [7,17]. Applications such as phase-encoded optical sampling are insensitive to laser amplitude modulation and consider the random widening as negligible [7]. In the case of a mode-locked laser, although the pump-power fluctuation induces both amplitude modulation and jitter, cavity-length fluctuation induces only phase noise [18]. In the domain of fiber-optic communications, this simplified model applies to the pulse-point modulation [23]. In this case, the sequence $\{J_n\}_{n\in\mathbb{Z}}$ takes values on a discrete and finite set. This property does not modify the power spectrum shape derived in this paper. Note that the influence of jitter on the uniform sampling of random processes has been already studied in Refs. [24,25].

The Independent Jitter Case

In Ref. [7], for instance, the considered model only involves jitter with a stationary or cyclostationary white noise distribution. Assume that $\{J_n\}_{n\in\mathbb{Z}}$ is an independent and identically distributed sequence. The intensity power spectrum derivation requires the knowledge of the exact distribution of the random variable J_n. Let $\psi(\omega)$ denote the jitter characteristic function

$$\psi(\omega) = E[e^{i\omega J_n}].$$

The power spectrum of the intensity consists of the two following terms:

$$\begin{cases} s_B(\omega) = & \frac{1}{2\pi}[|\widetilde{f}|^2.(1-|\psi|^2)](\omega), \\ s_L(\omega) = & \sum_{n=-\infty}^{\infty}[|\widetilde{f}.\psi|^2](2\pi n)\delta(\omega - 2\pi n). \end{cases} \tag{15}$$

As an example, consider a Gaussian shape function and a Gaussian jitter distribution defined, respectively, by

$$f(t) = \frac{1}{a\sqrt{2\pi}}\exp[-t^2/2a^2], \tag{16}$$

$$\psi(\omega) = \exp[-(b\omega)^2/2]. \tag{17}$$

In this case, the pulse shape is not of compact support but is characterized by its average full width at half-maximum T_{FWHM} defined by [8]

$$f\left(\frac{t}{T_{\mathrm{FWHM}}}\right) = \exp\left[-\left(\frac{t}{1.2T_{\mathrm{FWHM}}}\right)^2\right].$$

T_{FWHM} is simply related to parameter a. Equation (16) defines a Gaussian shape with unit area as required by Eq. (2). Equation (17) defines J_n as a centered Gaussian random variable with variance $1/b^2$, where $1/b$ is called the jitter strength. Under these specifications, the general spectrum expression Eq. (9) leads to

$$\begin{cases} s_B(\omega) = & \frac{1}{2\pi}(1-\exp[-(b\omega)^2])\exp[-(a\omega)^2], \\ s_L(\omega) = & \sum_{n=-\infty}^{\infty}\exp[-(a^2+b^2)(2\pi n)^2]\delta(\omega - 2\pi n). \end{cases} \tag{18}$$

First, the jitter contributes to the line spectrum decrease and a high jitter strength leads to a high band-spectrum magnitude. Moreover, $s_B(\omega)$ is an increasing function of ω for ω in the interval $\left[0, \frac{1}{a}\sqrt{\gamma\ln\left(1+\frac{1}{\gamma}\right)}\right]$ with $\gamma = \left(\frac{a}{b}\right)$. In this interval, $s_B(\omega)$ increases from 0 to $\frac{1}{2\pi}\frac{(1+\frac{1}{\gamma})^{-\gamma}}{1+\gamma}$. The length of the interval reduces when γ increases. This property allows us to discriminate the jitter from amplitude or width modulations. Indeed, the effect of amplitude or width modulations is a decreasing function of ω at low frequencies as demonstrated by experiments in Ref. [10], for instance. Figure 4 displays the optical pulse train intensity power spectrum in the case of independent Gaussian jitter only with Gaussian pulse shape. This spectrum differs from the spectra obtained in Figs. 2 and 3 for the

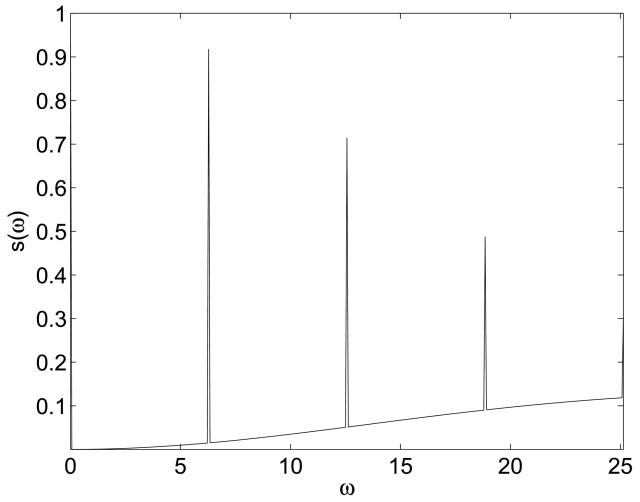

Fig. 4. Intensity power spectrum (first four harmonics) of an optical pulse train submitted to independent jitter of strength $1/b$ and Gaussian distribution with variance a^2 ($\Delta t = 10^{-3}$, $T = 1$, $a = 0.01$, $b = 0.05$).

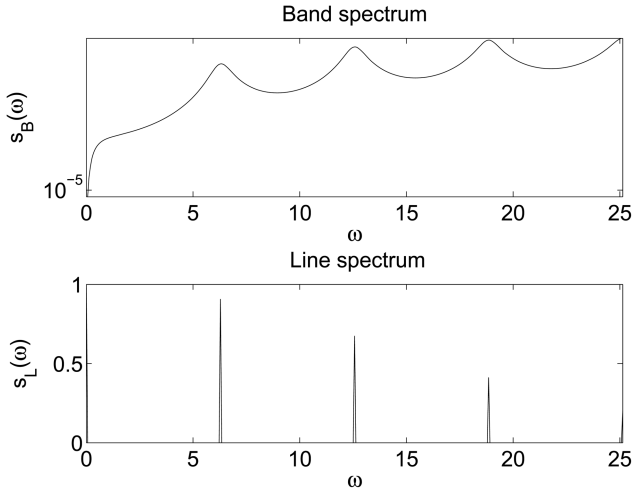

Fig. 5. Intensity power spectrum (first four harmonics) of an optical pulse train submitted to dependent jitter with Gaussian distribution of variance a^2 and exponential correlation $r_n = b^2 e^{-\nu|n|}$ ($\Delta t = 10^{-3}$, $T = 1$, $a = 0.001$, $b = 0.005$, $\nu = 0.5$).

amplitude modulation case. Indeed, a fast line spectrum decrease can be observed with a simultaneous band spectrum increase. As shown in Fig. 5, a quantitative jitter characterization can be performed by plotting the ratio of the noise band power and the harmonic amplitude as a function of the harmonic order; an increasing noise band contribution constitutes direct evidence of jitter [6].

The Dependent Jitter Case

When the J_n's are correlated, the line spectrum is unchanged since it is a function of $\psi(\omega)$ only. On the other hand, the band spectrum is a function of the following characteristic function:

$$\phi_n(\omega) = E[e^{i\omega(J_m - J_{n+m})}].$$

Consequently, the band-spectrum derivation requires knowledge of the two-dimensional jitter distribution [26]. When $\{J_n,\ n \in \mathbb{Z}\}$ is a stationary zero mean Gaussian sequence with $E[J_m J_{m+n}] = b^2 r_n$, $n \in \mathbb{Z}$, the band spectrum is given by

$$s_B(\omega) = \frac{1}{2\pi}\exp[-(a^2 + b^2)\omega^2] \times \sum_{n=-\infty}^{\infty} (\exp[r_n(b\omega)^2] - 1)e^{in\omega}. \quad (19)$$

Figure 5 displays the band and line spectrum in the case of dependent jitter with an exponential correlation $r_n = b^2 e^{-\nu|n|}$ with $b = 0.005$ and $v = 0.5$. The Gaussian pulse is characterized by $a = 0.001$. The simultaneous line spectrum decrease and band spectrum increase can clearly be observed in this figure. The ratio between the consecutive line heights denoted as Δs_L and the band spectrum for $\omega = 2\pi l$, $l \in \mathbb{Z}$ is given by

$$\gamma(l) = \left[\frac{\Delta s_L}{s_B}\right](2\pi l) = \left(\frac{1}{2\pi}\sum_{n=-\infty}^{\infty}(\exp[r_n(b2\pi l)^2] - 1)\right)^{-1}.$$

When r_n is a positive sequence, this ratio decreases with l, and goes to 0 when l goes to infinity as displayed in Fig. 6. Consequently, the jitter prevails for large-order harmonics. Conversely, the jitter in the first-order harmonics ($l = 1, 2$, up to several tens) and particularly for $l = 0$ can be neglected in physical situations [6].

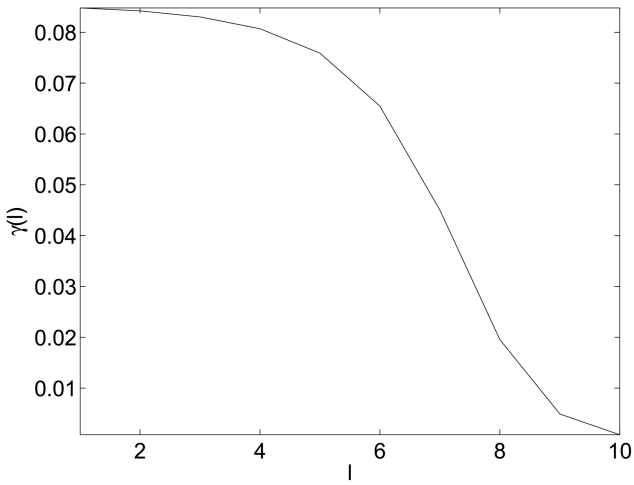

Fig. 6. Ratio between the consecutive line heights and the band spectrum (first 10 harmonics) in the case of dependent jitter ($\Delta t = 10^{-3}$, $T = 1$, $a = 0.001$, $b = 0.005$, $\nu = 0.5$).

C. The Independent Width Modulation Case

The pure width modulation model assumes $A_n = 1$, $J_n = 0$ with probability 1, $E[W_n] = 1$, $Var[W_n] = \sigma_W^2 > 0$, and $\Pr[W_n \geq c] = 1$ for some $c > 0$. Such a model relates to pulse-width modulation or pulse-duration modulation in the field of communications [20,21] and sampling [27]. For this reason, independence of the width modulation sequence is assumed. According to the literature, the width modulation is not directly characterized from the intensity power spectrum in the other mentioned application fields. Indeed, width modulation is rather detected through energy fluctuations of the second harmonic of the laser output [6]. The noise in the second harmonic is much stronger, with a frequency band twice as large and with a different bimodal shape only [6]. This property can only be explained by the presence of width modulation. Moreover, in such applications width modulation correlation is in the form of some strongly damped oscillation, suggesting oscillatory changes [6]. This subsection focusses on the telecommunication model (independent width modulation) and on the direct analysis of the intensity power spectrum. When the sequence W_n is independent and identically distributed, the derivation of the intensity power spectrum requires knowledge of the characteristic function ψ of $V_n = \frac{1}{W_n} - 1$:

$$\psi(\omega) = E[e^{i\omega V_n}].$$

Because the W_n's are independent, the band spectrum in Eq. (9) reduces to $\frac{1}{2\pi}\tilde{\beta}_0^0(\omega)$ like in the examples above. It is difficult to provide a general closed-form formula like in the independent amplitude modulation case, Eq. (13), or the independent jitter case, Eq. (15). An approximation is derived from the general expression under the hypothesis of small fluctuations. Consider the case of a unit area Gaussian pulse, Eq. (16), and of a binary pulse-width modulation defined by

$$\Pr[V_n = v] = \Pr[V_n = -v] = \frac{1}{2}.$$

The intensity power spectrum derivation leads to the following expressions:

$$\begin{cases} s_B(\omega) = \frac{1}{8\pi}\left(\frac{1}{1+v}\exp\left[-\frac{1}{2}\left(\frac{a\omega}{1+v}\right)^2\right] - \frac{1}{1-v}\exp\left[-\frac{1}{2}\left(\frac{a\omega}{1-v}\right)^2\right]\right)^2, \\ s_L(\omega) = \sum_{n=-\infty}^{\infty}\frac{1}{4}\left(\frac{1}{1+v}\exp\left[-\frac{1}{2}\left(\frac{2\pi n a}{1+v}\right)^2\right] + \frac{1}{1-v}\exp\left[-\frac{1}{2}\left(\frac{2\pi n a}{1-v}\right)^2\right]\right)^2\delta(\omega - 2n\pi). \end{cases}$$

In experiments of Ref. [11], the product $a\omega$ goes from 0 to a few units. Since v is in the same range as a, an approximation of the band spectrum for small v yields

$$s_B(\omega) \cong \frac{v^2}{2\pi}e^{-(a\omega)^2}(1-(a\omega)^2)^2.$$

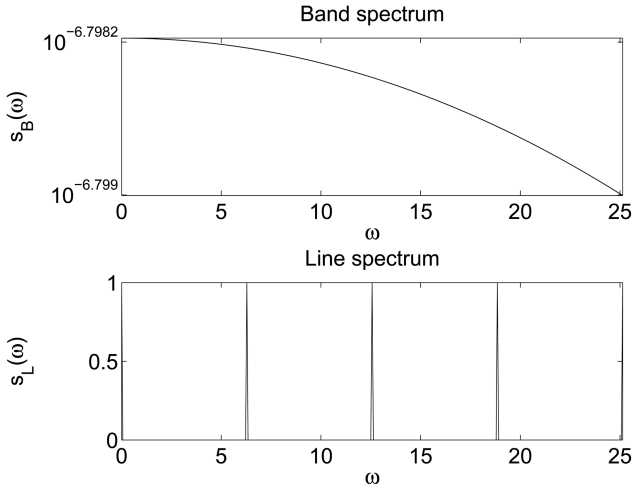

Fig. 7. The intensity power spectrum (first four harmonics) of an optical pulse train submitted to independent width modulation ($\Delta t = 10^{-3}$, $T = 1$, $a = 0.001$, $v = 0.001$).

Like in the amplitude modulation case, $s_B(\omega)$ is a decreasing function of $a\omega$. For larger values of v, $s_B(\omega)$ can be shown to be a decreasing function of $a\omega$ in the low frequency region (note that the ranges of the band and line spectra are different since one is homogeneous to the derivative of a power, whereas the other is homogeneous to the power itself). Figure 7 displays the band and line spectra in the case of an independent width modulation with $a = 0,001$ and $v = 0,001$. This figure clearly illustrates the band spectrum decrease associated with an approximately constant line spectrum.

5. Conclusion

The general expression of the spectrum of a noisy optical pulse train submitted to jitter, as well as amplitude and width modulation, has been provided. The proposed general model of the optical pulse train allows us to take into account the three types of fluctuations with arbitrary distribution and possible cross correlation, as well as arbitrary pulse shapes. Simplified expressions in particular cases of interest have been derived. These expressions are in qualitative agreement with the results obtained by experimental measurements in the literature. The obtained theoretical expressions explain some experimental observations (for instance the different behavior of jitter and amplitude modulation

as a function of frequency), as well as various approximations in particular measurement frequency and fluctuation amplitude ranges.

Appendix A

This appendix justifies some assumptions of the pulse-shape function. Let t_0 denote a shift parameter such that $f(t-t_0)$ is centered on the middle of the first time period $[0,1]$. Let m_f and w_f denote, respectively, $f(t)$ barycenter and time dispersion:

$$\int_{-\infty}^{\infty} tf(t)\mathrm{d}t = m_f, \quad \int_{-\infty}^{\infty}(t-m_f)^2 f(t)\mathrm{d}t = w_f^2. \quad \text{(A20)}$$

Consider the translated and scaled shape function $f\left(\frac{t-a}{b}\right)$ with $a,\ b>0$. The intensity normalization condition (2) and the Eq. (A20) become:

$$\int_{-\infty}^{\infty} f\left(\frac{t-a}{b}\right)\mathrm{d}t = b, \quad \frac{1}{b}\int_{-\infty}^{\infty} tf\left(\frac{t-a}{b}\right)\mathrm{d}t = a + bm_f,$$
$$\frac{1}{b}\int_{-\infty}^{\infty}(t-a-bm_f)^2 f\left(\frac{t-a}{b}\right)\mathrm{d}t = (bw_f)^2.$$

The time-axis affine transformation defined by $t \to \frac{t-a}{b}$ leads to a pulse barycenter translation with parameter $a+(b-1)m_f$ and a pulse scaling with parameter b. A barycenter translation of parameter a for any b is obtained if the pulse function is such that $m_f = 0$.

Appendix B

If Φ is uniformly distributed over $[0,1]$ and independent of the real process $I(t)$, then $\tilde{I}(t) = I(t+\Phi)$ is a stationarized version of $I(t)$ and

$$E[\mathrm{I}\check{}(t)\mathrm{I}\check{}(t+\tau)] = \int_0^1 E[I(t+\phi)I(t+\tau+\phi)]\mathrm{d}\phi. \quad \text{(B21)}$$

$E[I(t+\phi)I(t+\tau+\phi)]$ is periodic with period 1 with respect to ϕ, and then, using Eqs. (7) and (8)

$$\begin{aligned} E[\mathrm{I}\check{}(t)\mathrm{I}\check{}(t+\tau)] &= \int_0^1 E[I(\phi)I(\tau+\phi)]d\phi \\ &= \int_0^1 \beta_{\overline{\phi+\tau}}(\phi,\underline{\phi}+\tau)d\phi \\ &= \int_0^1 \beta^0_{\overline{\phi+\tau}}(\phi,\underline{\phi}+\tau)d\phi \\ &\quad + \int_0^1 \alpha(\phi)\alpha(\underline{\phi}+\tau)d\phi. \end{aligned}$$

According to Eq. (8), the first integral will give rise to band spectrum $s_B(\omega)$ and the second integral, as a periodic function of τ, will lead to line spectrum $s_L(\omega)$ by the Fourier transform of Eq. (B21). Indeed, a periodic function of τ, the first integral can be expanded in a Fourier series:

$$\int_0^1 \alpha(\phi)\alpha(\underline{\phi}+\tau)d\phi = \sum_{n=-\infty}^{\infty} |\tilde{\alpha}(2\pi n)|^2 e^{2i\pi n\tau}. \quad \text{(B22)}$$

The one-dimensional Fourier transform of this expression gives rise to the line spectrum:

$$s_L(\omega) = \sum_{n=-\infty}^{\infty} |\tilde{\alpha}(2\pi n)|^2 \delta(\omega - 2\pi n).$$

A variable change (of the form $-n+\phi+\tau=\tau'$) is performed on the second integral term before deriving its Fourier transform:

$$s_B(\omega) = \frac{1}{2\pi}\int_{-\infty}^{\infty}\left[\int_0^1 \beta^0_{\overline{\phi+\tau}}(\phi,\underline{\phi}+\tau)d\phi\right]e^{-i\omega\tau}\mathrm{d}\tau \quad \text{(B23)}$$

$$= \frac{1}{2\pi}\int_0^1\left[\sum_{n=-\infty}^{\infty}\int_{n-\phi}^{n+1-\phi}\beta^0_{\overline{\phi+\tau}}(\phi,\underline{\phi}+\tau)e^{-i\omega\tau}\mathrm{d}\tau\right]\mathrm{d}\phi \quad \text{(B24)}$$

$$= \frac{1}{2\pi}\sum_{n=-\infty}^{\infty} e^{-i\omega n}\iint_{(0,1)^2}\beta^0_n(\phi,\tau)e^{-i\omega(\tau-\phi)}\mathrm{d}\tau\mathrm{d}\phi \quad \text{(B25)}$$

$$= \frac{1}{2\pi}\sum_{n=-\infty}^{\infty} e^{i\omega n}\tilde{\beta}^0_n(\omega). \quad \text{(B26)}$$

References

1. J. M. Arnold, A. D. Boardman, H. M. Mehta, and R. C. J. Putman, "PPM soliton pulse trains in optical fibers," Opt. Commun. **122**, 48–57 (1995).
2. S. Y. Suh, "Pulse width modulation for analog fiber-optic communications," J. Lightwave Technol. **5**, 109–112 (1987).
3. G. L. Carr, R. P. S. M. Lobo, C. J. Hirschmugl, J. LaVeigne, D. H. Reitze, and D. B. Tanner, "Time resolved spectroscopy using synchroton infrared pulses," Proc. SPIE **3153**, 80–86 1997.
4. R. Hofman and H. Pfeiderer, "Electro-optic sampling system for the testing of high-speed integrated circuits using a free running solid-state laser," J. Lightwave Technol. **14**, 1788–1793 (1996).
5. T. Debuisschert, "Nanosecond optical oscillators," Quantum Semiclass. Opt. **9**, 209–219 (1997).
6. D. von der Linde, "Characterization of the noise in continuously operating mode-locked lasers," Appl. Phys. B **39**, 201–217 (1986).
7. P. W. Juodawlkis, J. C. Twichell, J. L. Wasserman, G. E. Betts, and R. C. Williamson, "Measurement of mode-locked laser

timing jitter by use of phase-encoded optical sampling," Opt. Lett. **26**, 289–291 (2001).
8. L. P. Chen, "Spectral measurement of the noise in continuous-wave mode-locked laser pulses," IEEE J. Quantum Electron. **32**, 1817–1825 (1996).
9. I. G. Fuss and K. J. Grant, "An all frequency model of optical pulse train noise," Opt. Quantum Electron. **31**, 431–449 (1999).
10. O. Pottiez, O. Deparis, R. Kiyan, P. Mégret, and M. Blondel, "Measurement of pulse width and amplitude jitter noises of gigahertz optical pulse train by time-domain demodulation," Opt. Lett. **26**, 1779–1781 (2001).
11. K. J. Grant, "Spectral technique for measuring the pulse-width jitter of a gain-switched laser," Opt. Commun. **213**, 183–186 (2002).
12. D. Henderson and A. G. Roddie, "A comparison of spectral and temporal techniques for the measurement oftiming jitter and their application in a modelocked argon ion and dye laser system," Opt. Commun. **100**, 456–460 (1993).
13. A. Papoulis, *Probability, Random Variables, and Stochastic Processes* (McGraw-Hill, 1991).
14. H. Cramer and M. R. Leadbetter, *Stationary and Related Processes* (Wiley, 1967).
15. J. L. Doob, *Stochastic Processes* (Wiley, 1953).
16. B. Lacaze, "Calculation of power spectra for processes with cyclostationary characteristics," in French, Traitement du Signal **14**, 64–71 (1997).
17. H. Tsuchida, "Wideband phase-noise measuremant of mode-locked laser pulses by a modulation technique," Opt. Lett. **23**, 286–288 (1998).
18. H. Tsuchida, "Correlation between amplitude and phase noise in a mode-locked Cr:LiSAF laser," Opt. Lett. **23**, 1686–1688 (1998).
19. H. Tsuchida, "Time-interval analysis of laser-pulse-timing fluctuations," Opt. Lett. **24**, 1434–1436 (1999).
20. L. E. Franks, *Signal Theory* (Prentice-Hall, 1969).
21. J. Proakis, *Digital Communications* (McGraw-Hill, 1989).
22. B. H. Kolner and D. M. Bloom, "Electrooptic sampling in GaAs integrated circuits," IEEE J. Quantum Electron. **22**, 79–93 (1986).
23. J. M. H. Elmirghani and R. A. Cryan, "Timing jitter and its impact on a self-synchronized optical fiber PPM system," European J. Telecom. **6**, 161–170 (1995).
24. B. Lacaze, "Reconstruction of stationary processes sampled at random times," in *Nonuniform Sampling-Theory and Practice*, E. Marvasti, ed. (Plenum, 2001), pp. 361–390.
25. C. Mailhes and B. Lacaze, "Jitter effects in multipath environment" ICASSP, Salt Lake City VI (IEEE, 2001), pp. 3905–3908.
26. B. Lacaze, "Stationary clock changes on stationary processes," Signal Processing **55**, 191–205 (1996).
27. B. Lacaze and C. Mailhes, "Influence of a random integration width on periodic sampling," ICASSP HongKong II (IEEE, 2002), pp. 1189–1192.